



THE UNIVERSITY *of* EDINBURGH

Edinburgh Research Explorer

A New Family of High Oxidation State Antiperovskite Nitrides

La_3MN_5 (M=Cr, Mn and Mo)

Citation for published version:

Yuan, Y, Yang, M, Kloß, SD & Attfield, JP 2024, 'A New Family of High Oxidation State Antiperovskite Nitrides: La_3MN_5 (M=Cr, Mn and Mo)', *Angewandte Chemie - International Edition*.
<https://doi.org/10.1002/anie.202405498>

Digital Object Identifier (DOI):

[10.1002/anie.202405498](https://doi.org/10.1002/anie.202405498)

Link:

[Link to publication record in Edinburgh Research Explorer](#)

Document Version:

Publisher's PDF, also known as Version of record

Published In:

Angewandte Chemie - International Edition

General rights

Copyright for the publications made accessible via the Edinburgh Research Explorer is retained by the author(s) and / or other copyright owners and it is a condition of accessing these publications that users recognise and abide by the legal requirements associated with these rights.

Take down policy

The University of Edinburgh has made every reasonable effort to ensure that Edinburgh Research Explorer content complies with UK legislation. If you believe that the public display of this file breaches copyright please contact openaccess@ed.ac.uk providing details, and we will remove access to the work immediately and investigate your claim.



Nitride Antiperovskites

A New Family of High Oxidation State Antiperovskite Nitrides: La_3MN_5 (M=Cr, Mn and Mo)

Yao Yuan, Minghui Yang, Simon D. Klotz, and J. Paul Attfield*

Abstract: Three new nitrides La_3MN_5 (M=Cr, Mn, and Mo) have been synthesized using a high pressure azide route. These are the first examples of ternary Cs_3CoCl_5 -type nitrides, and show that this $(\text{MN}_4)\text{NLa}_3$ antiperovskite structure type may be used to stabilise high oxidation-state transition metals in tetrahedral molecular $[\text{MN}_4]^{n-}$ nitridometallate anions. Magnetic measurements confirm that Cr and Mo are in the M^{6+} state, but the M=Mn phase has an anomalously small paramagnetic moment and large cell volume. Neutron powder diffraction data are fitted using an anion-excess $\text{La}_3\text{MnN}_{5.30}$ model (space group $I4/mcm$, $a=6.81587(9)$ Å and $c=11.22664(18)$ Å at 200 K) in which Mn is close to the +7 state. Excess-anion incorporation into Cs_3CoCl_5 -type materials has not been previously reported, and this or other substitution mechanisms may enable many other high oxidation state transition metal nitrides to be prepared.

Introduction

Transition metal oxides have many important properties and a diverse chemistry reflecting the stabilisation of a wide range of oxidation states, e.g. from +2 in $\text{K}_2\text{Mn}_2\text{O}_3$ up to +7 in KMnO_4 for manganese. High oxidation state transition metals in nitrides are however much rarer as synthesis of nitrogen-rich materials is impeded by unfavourable nitride thermodynamics due to the stability of the $\text{N}\equiv\text{N}$ triple bond

(947 kJ mol^{-1}) and inertness of the N_2 molecule.^[1] Hence transition metal nitrides, which have wide-ranging applications in ceramics, optoelectronics, and phosphors,^[2] tend to be limited to low oxidation states.^[3]

A recent development in the synthesis of transition metal nitrides with high oxidation states involves the use of sodium azide (NaN_3) as the nitrogen source in high-pressure high-temperature (HPHT) reactions. The decomposition of NaN_3 during the reaction results in a high nitrogen activity while metallic sodium can serve as a flux facilitating the synthesis process. This method has been successfully applied in the preparation of compounds such as Ca_4FeN_4 (containing $[\text{FeN}_3]^{5-}$ anions),^[4] Ca_2NiN_2 ,^[5] and the perovskite LaReN_3 .^[6] Perovskite-type nitrides of other heavy transition metals have also been grown as thin films for LaWN_3 ^[7] and CeMN_3 (M=Mo and W).^[8]

We subsequently explored HPHT azide synthesis of the possible first row transition metal nitride LaMnN_3 . This perovskite was not obtained, however, a new phase was observed and identified as La_3MnN_5 , the first nitride adopting the Cs_3CoCl_5 -type structure, which may be described as a molecular antiperovskite arrangement. We have also explored the Cr and Mo analogues, and the synthesis, structures and magnetic measurements for the M=Cr, Mn and Mo members of this new La_3MN_5 family of high oxidation state transition metal nitrides are reported here.

Results and Discussion

La_3MN_5 phases were synthesized by subjecting mixtures of M (=Cr, Mn or Mo) metal, LaN , and NaN_3 powders in a 1:3:2 ratio to HPHT conditions at 1000 °C and 8 GPa. The resulting products were characterized by powder X-ray diffraction (XRD), which revealed the formation of new Cs_3CoCl_5 -type phases as shown in Figure 1. All three samples appeared as dark grey powders and were sensitive to moisture and air. Traces of secondary phases were observed for M=Mn and Mo samples. More substantial impurity was found for M=Cr and this was not eliminated by varying reaction conditions.

XRD patterns for the La_3MN_5 (M=Cr, Mn and Mo) products were indexed on body-centred tetragonal unit cells with lattice parameters $a\approx 6.8$ and $c\approx 11$ Å. Good Rietveld fits were obtained with a Cs_3CoCl_5 -type structural model in space group $I4/mcm$ as shown in Figure 1.^[9] Cell parameters and other results are shown in Table 1 with full refinement models shown in SI. No evidence of sodium substitution at

[*] Dr. Y. Yuan, Prof. J. P. Attfield
 Centre for Science at Extreme Conditions and School of Chemistry
 University of Edinburgh
 Peter Guthrie Tait Road, EH9 3FD, Edinburgh, UK
 E-mail: j.p.attfield@ed.ac.uk

Prof. M. Yang
 School of Environmental Science and Technology
 Dalian University of Technology
 No. 2 Linggong Road, 116024, Dalian, China

Dr. S. D. Klotz
 Department of Chemistry
 Ludwig-Maximilians-Universität München
 Butenandtstr. 5–13, 81377 Munich, Germany

© 2024 The Authors. Angewandte Chemie International Edition published by Wiley-VCH GmbH. This is an open access article under the terms of the Creative Commons Attribution License, which permits use, distribution and reproduction in any medium, provided the original work is properly cited.

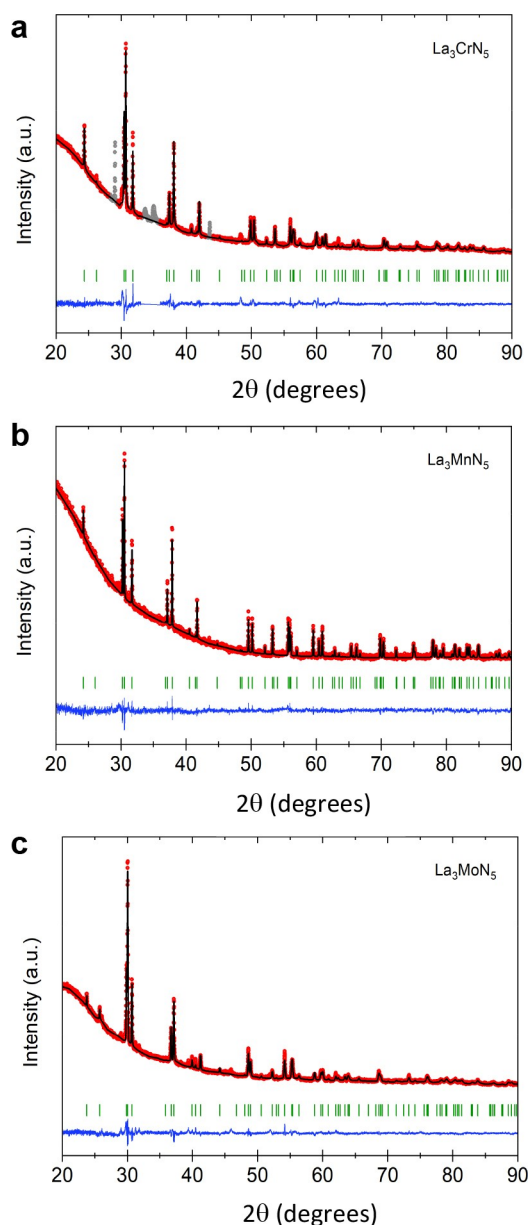


Figure 1. Rietveld fits of the Cs_3CoCl_5 -type structure to room temperature $\text{Cu-K}\alpha_1$ powder X-ray diffraction data for (a) La_3CrN_5 , (b) La_3MnN_5 , and (c) La_3MoN_5 samples. Impurity peaks (grey points) have been excluded from the fit in (a).

Table 1: Unit cell parameters and N–La distances and angles from Rietveld fits of a tetragonal Cs_3CoCl_5 -type model (space group $I4/mcm$) to room temperature XRD data for the La_3MN_5 phases (M=Mn, Cr, Mo).

M	Mn	Cr	Mo
a (Å)	6.84658(5)	6.79775(9)	6.91895(9)
c (Å)	11.28748(10)	11.25319(17)	11.64246(17)
Volume (Å ³)	529.109(7)	520.002(13)	557.346(14)
(N1–La1) $\times 4$ (Å)	2.532(1)	2.521(1)	2.555(1)
(N1–La2) $\times 2$ (Å)	2.8219(1)	2.8133(1)	2.9106(1)
(N1–La1–N1) (°)	145.85(6)	144.84(6)	146.52(6)
(N1–La2–N1) (°)	180	180	180

La or M sites was observed, consistent with findings from previous studies.^[4–6]

The XRD refinements confirm that new La_3MN_5 (M=Cr, Mn and Mo) phases have been recovered from HPHT synthesis. They may be described as $(\text{MN}_4)\text{NLa}_3$ molecular antiperovskites in the standard ABX_3 perovskite formulation, with tetrahedral $[\text{MN}_4]^{6-}$ anions at the A-sites within a network of corner-sharing NLa_6 octahedra. The highest possible space group symmetry for such $(\text{MX}_4)\text{XM}'_3$ antiperovskites is cubic $P\bar{4}3m$ if the MX_4 tetrahedra are ordered, but this structure is not reported for any literature materials, and they are stabilized by octahedral rotations giving the tetragonal $I4/mcm$ Cs_3CoCl_5 -type arrangement. It was not possible to obtain reliable M–N distances from the XRD refinements but La positions within the BX_3 ($\text{N1La}_2\text{La}_2$) network were refined accurately to give the N1–La distances and N1–La–N1 angles shown in Table 1. The NLa_6 octahedra are strongly elongated in the c -direction and are rotated by $\sim 17^\circ$ around the c -axis.

Ionic radii for 4-coordinate cations are in order $r(\text{M}^{6+}) = \text{Mn} (0.255) < \text{Cr} (0.26) < \text{Mo} (0.41 \text{ \AA})$ ^[10] so the cell volume for La_3MnN_5 is anomalously large in comparison to that for La_3CrN_5 . This evidences some off-stoichiometry such as incorporation of additional nitride anions, consistent with magnetic and neutron diffraction results later.

Magnetic susceptibility (χ) measurements for the La_3MN_5 (M=Cr, Mn and Mo) samples at variable temperature, and magnetisation (M)–field (H) hysteresis loops at 2 and 300 K are shown in Figure 2. The susceptibility data show a high background contribution which likely reflects the temperature independent paramagnetism of high valent transition metal ions as well as Pauli paramagnetism from any metal or low valent metal nitride impurities. Features emerging below 250 K for M=Mn and 175 K for M=Mo are attributed to ferromagnetic impurities. The low temperature Curie tails evidence localised-electron paramagnetism from the La_3MN_5 phases or impurities, and were fitted as a sum of a Curie–Weiss and a constant term; $\chi = C/(T-\theta) + A$ to the inverse susceptibilities as shown in Figure 2. The extracted magnetic parameters are presented in Table 2. Small negative Weiss temperatures (θ) imply that the observed paramagnetism comes from the main phase with weak antiferromagnetic interactions between spins in isolated $[\text{MN}_4]^n$ tetrahedra.

Paramagnetic moments are known to be a sensitive measure of oxidation state for tetrahedral $[\text{MX}_4]^n$ anions of high valent transition metals. Reported values for d^1 ($1.65 \mu_B$ for K_3CrO_4 ; 1.75 – $1.83 \mu_B$ for K_2MnO_4 and BaMnO_4) and d^2

Table 2: Fitted magnetic parameters (Curie constant, paramagnetic moment, Weiss temperature and constant term) for the La_3MN_5 samples.

M	Mn	Cr	Mo
C ($\text{emu} \cdot \text{K} \cdot \text{mol}^{-1}$)	0.109(4)	0.0208(3)	0.0122(6)
μ_{para} (μ_B)	0.93	0.41	0.31
θ (K)	−4.4(5)	−1.6(2)	−3.7(6)
A ($\text{emu} \cdot \text{mol}^{-1}$)	0.0021	0.0016	0.0009

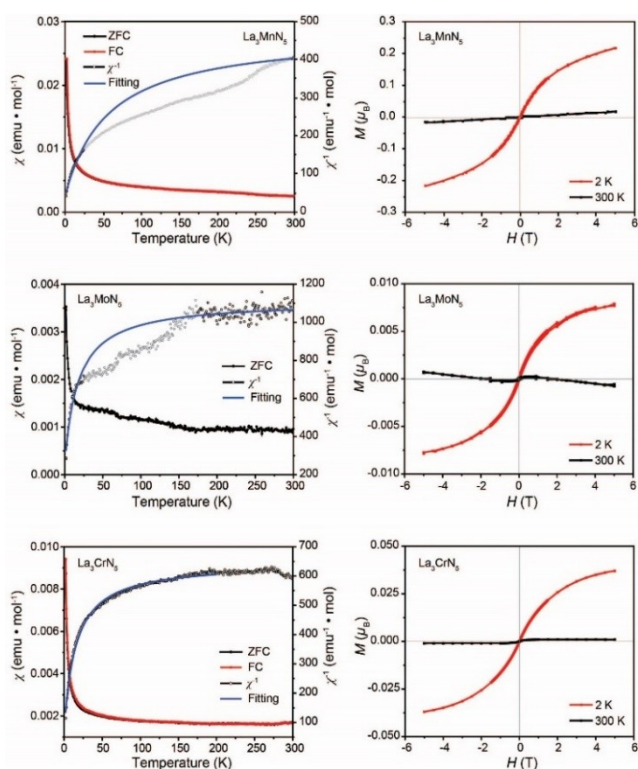


Figure 2. Magnetisation plots for La_3MN_5 samples (a,b) $\text{M}=\text{Mn}$, (c,d) $\text{M}=\text{Mo}$, (e,f) $\text{M}=\text{Cr}$. (a,c,e) Zero field cooled (ZFC) and field cooled (FC) molar magnetic susceptibilities and inverse ZFC susceptibility in a field of 0.1 T with a fit of the function shown in the text to low temperature inverse susceptibility points. (b,d,f) Magnetisation-field hysteresis loops measured at 2 and 300 K.

($2.83 \mu_{\text{B}}$ for K_3MnO_4 ; $2.79 \mu_{\text{B}}$ for Li_7MnN_4) cations^[11,12] closely follow the expected variation of spin-only moments $0 \rightarrow 1.73 \rightarrow 2.83 \mu_{\text{B}}$ for $0 \rightarrow 1 \rightarrow 2$ d-electrons. Hence the paramagnetic moments of the La_3MN_5 phases are taken to be a good measure of oxidation state in their $[\text{MN}_4]^{n-}$ ($\text{M}=\text{Cr}$, Mn and Mo) anions.

$[\text{MN}_4]^{6-}$ ($\text{M}=\text{Cr}$ and Mo) anions are diamagnetic d^0 species so the observed paramagnetism may be due to impurity phases or off-stoichiometry. The 300 K M - H loops show that at high H , M has a small, almost constant positive value for $\text{M}=\text{Cr}$ and a negative slope and values for $\text{M}=\text{Mo}$, consistent with intrinsic diamagnetism, although a small paramagnetic contribution is seen at low H and this increases to dominate the M - H plot at 2 K. The fitted low temperature Curie terms C and derived paramagnetic moments shown in Table 2, correspond to 5.6 % and 3.2 % of a spin-only d^1 impurity for the $\text{M}=\text{Cr}$ and Mo samples respectively. If attributed to the La_3MN_5 -type phases then these contributions imply respective oxidation states of $\text{Cr}^{5.94+}$ and $\text{Mo}^{5.97+}$. Hence La_3CrN_5 and La_3MoN_5 are confirmed as being essentially stoichiometric nitrides of these metals in their +6 states, despite the presence of a secondary phase (which is presumably non-magnetic) in the La_3CrN_5 sample.

Stoichiometric La_3MnN_5 would contain $d^1 \text{Mn}^{6+}$ and so a paramagnetic moment $\sim 1.7 \mu_{\text{B}}$ would be expected. However,

the observed moment of $0.93 \mu_{\text{B}}$ is substantially reduced, corresponding to just 29 % spin-only d^1 ions per Mn. This implies that La_3MnN_5 is substantially off-stoichiometric with Mn further oxidised to an average +6.71 oxidation state. This would be consistent with the composition $\text{La}_3\text{MnN}_{5.24}$ if extra nitride anions are incorporated as suggested by the anomalous cell volume for La_3MnN_5 noted above and the following neutron diffraction analysis.

A neutron powder diffraction refinement of the structure of La_3MnN_5 was performed to obtain precise N atom positions and investigate off-stoichiometry evidenced by the anomalously large cell volume and small paramagnetic moment. Initial free refinement of the nitride site occupancies gave 65.8(8) and 99.2(6) % N occupancy at N1 and N2 positions, respectively. This demonstrates that N2 sites which are coordinated to Mn are fully occupied and hence that stoichiometric $[\text{MnN}_4]^{n-}$ anions are present, and the N2 occupancy was subsequently fixed at 100 %. The deficiency of scattering at the N1 site indicates that the sample is off-stoichiometric with nitride vacancies (V) or substitution of nitrogen (scattering length $b_{\text{N}}=9.36 \text{ fm}$) by oxygen ($b_{\text{O}}=5.83 \text{ fm}$) due to possible air exposure occurring. The observed N1 site scattering is equivalent to $\text{N}_{0.66}\text{V}_{0.34}$ or $\text{N}_{0.09}\text{O}_{0.91}$ average site occupancies. However, both possibilities would give an oxidation state near Mn^{5+} (d^2) which is inconsistent with the observed small paramagnetic moment.

A simple structural mechanism that resolves the observations of anomalous cell volume, reduced paramagnetic moment, and N1-site scattering deficiency for La_3MnN_5 is that additional nitride ions are incorporated into the Cs_2CoCl_5 -type structure under the HPHT synthesis conditions, forming clusters around vacant N1 sites. This was modelled by introducing an interstitial nitride N3 position close to N1, as shown in Table 3 and on Figure 3a. The minimal size of a defect cluster is for two N3 interstitials to replace a lattice N1, hence their populations were constrained in a ratio of $\text{N1}:\text{N3}=1-x:2x$ and the overall stoichiometry is $\text{La}_3\text{MnN}_{5+x}$. N3 lies on a general (x,y,z) position in space group $I4/mcm$ so the pair of N3 interstitials is disordered four ways around the high symmetry N1 vacancy at $(0, 0, 0)$ as shown on Figure 3a. A stable refinement of the N3 coordinates was obtained as shown in Table 3, giving the fit shown in Figure 3b and interatomic distances in Table 4. This excess-nitride $\text{La}_3\text{MnN}_{5+x}$ model gives a better fit to the neutron diffraction profile (weighted profile $R_{\text{wp}}=2.39 \%$, goodness-of-fit $\chi^2=10.8$) than a stoichiometric La_3MnN_5 model ($R_{\text{wp}}=2.62 \%$, $\chi^2=12.9$)

Table 3: Atomic parameters for the La_3MnN_5 sample refined against 200 K neutron powder diffraction data. ($I4/mcm$; $a=6.81587(9)$, $c=11.22664(18) \text{ \AA}$; residuals $R_{\text{p}}=1.79 \%$, $R_{\text{wp}}=2.39 \%$, $\chi^2=10.8$)

Atom	Site	x	y	z	Occ	$B_{\text{iso}} (\text{Å}^2)$
La1	8h	0.6724(2)	0.1724	0	1	0.53(3)
La2	4a	0	0	0.25	1	0.53
Mn1	4b	0	0.5	0.25	1	0.53
N1	4c	0	0	0	0.704(4)	0.64(2)
N2	16l	0.1435(1)	0.6435	0.1521(1)	1	0.64
N3	32m	0.025(2)	0.090(2)	0.053(1)	0.074	0.64

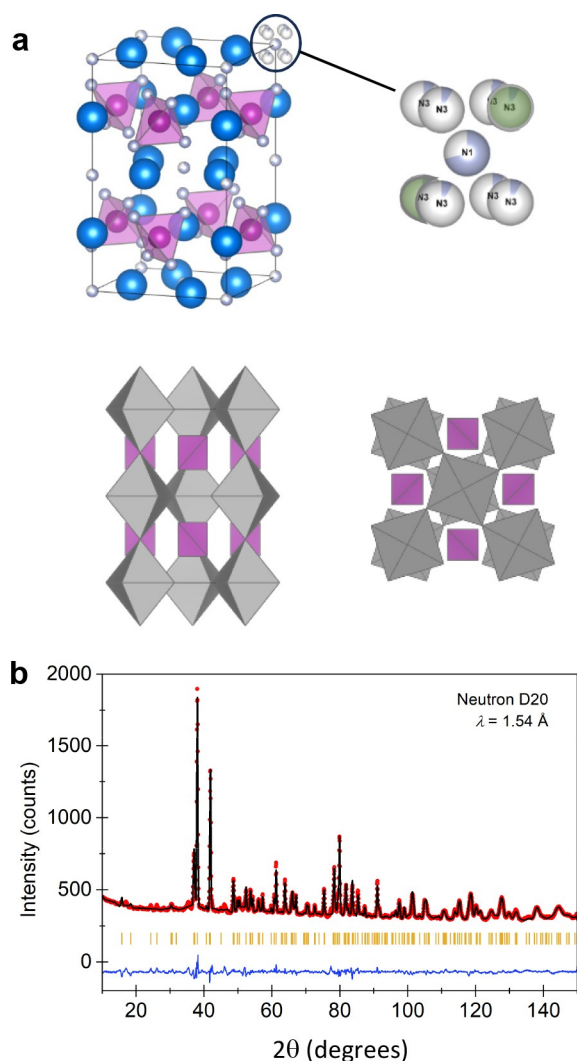


Figure 3. (a) Atomistic and polyhedral views of the La_3MnN_5 antiperovskite structure. Upper image shows the N3 positions for excess nitrides around one lattice N1 site with La/Mn/N atoms in blue/pink/grey. Defect clusters of two diagonally-opposite occupied N3 sites (one such pair is shaded green) surrounding a N1 vacancy enable excess nitride to be incorporated in the refined $\text{La}_3\text{MnN}_{5.3}$ composition. Polyhedral views projected on (010) left, and (001) right, planes show MnN_4 tetrahedra in pink and NLa_6 octahedra in grey. (b) Fit of the refined $\text{La}_3\text{MnN}_{5.3}$ model to powder neutron diffraction data at 200 K.

Table 4: Bond distances and angles for La_3MnN_5 from the neutron refinement at 200 K.

Length (Å)		Length (Å)	
La1–N1	2.523(1)	La2–N1	2.807(1)
La1–N2	2.463(2)/2.755(2)	La2–N2	2.841(1)
La1–N3	2.00(1)/2.54(1)/2.80(1)	La2–N3	2.30(1)
Mn–N2	1.767(1)	N3–N3	1.74(3)
Angle (°)		Angle (°)	
N1–La1–N1	145.51(6)	N2–Mn–N2	103.07(8)/112.77(7)
N1–La2–N1	180		

and it resolves the anomalies noted before, with good agreement between the value of the nitride excess $x = 0.296(4)$ from neutron refinement and $x = 0.24$ based on the paramagnetic moment. Hence our experimental observations support introduction of extra nitride ions as $\text{La}_3\text{MnN}_{5+x}$, charge-compensated by almost complete oxidation of Mn^{6+} to Mn^{7+} (full oxidation would give $x = 0.33$).

$[\text{Mn}^{6+}\text{N}_4]^{6-}$ and $[\text{Mn}^{7+}\text{N}_4]^{5-}$ anions have not previously been structurally characterized but the observed Mn–N2 distance of 1.767(1) Å for the $[\text{Mn}^{6.9+}\text{N}_4]^{5.1-}$ anion in $\text{La}_3\text{MnN}_{5.30}$ is consistent with values of 1.81–1.85 Å for $\text{Mn}^{5+}\text{N}_4^{7-}$ in Li_7MnN_4 ,^[12,13] allowing for the change in Mn oxidation state. Electrochemical delithiation of the latter material is reported to give $\text{Li}_{7-x}\text{MnN}_4$ products with x up to 1.7 demonstrating a comparably high $\text{Mn}^{6.7+}$ state to that in $\text{La}_3\text{MnN}_{5.30}$, but the products were not structurally characterised.^[13,14]

Additional nitride anions are incorporated into $\text{La}_3\text{MnN}_{5.30}$ through defect clusters which are modelled here by two occupied N3 sites surrounding an N1 vacancy as shown in Figure 3a. The N3 pairs are disordered over four possible orientations around each N1 vacancy. Some short (2.0–2.3 Å) La–N3 contacts to the defect sites are present as shown in Table 4 and the refined N3–N3 distance of 1.74(3) Å is also short, but is too long to indicate N–N bonding as distances in pernitrides such as LaN_2 and FeN_2 are between 1.2 and 1.5 Å.^[15] The short distances in $\text{La}_3\text{MnN}_{5.30}$ reflect the small (7.4%) statistical occupancy of the N3 site and local atomic displacements are likely to occur to relieve the close contacts. Similar short N–N distances are apparent in the average crystal structures of other interstitial rare earth transition metal nitrides, such as 1.70 Å between 12% occupied N sites in $\text{Nd}_2\text{Fe}_{17}\text{N}_{2.52}$.^[16]

The above results demonstrate that Cs_3CoCl_5 -type R_3MN_5 nitrides for rare earth $\text{R}=\text{La}$ and transition metals $\text{M}=\text{Cr}$, Mn and Mo have been synthesized at HPHT using the azide synthesis route. The tetragonal $I4/mcm$ Cs_3CoCl_5 -type structure is observed for many halides, hydrides e.g. K_3MnH_5 ,^[17] oxides e.g. Ba_3CrO_5 ,^[18] and sulphides e.g. $\text{BaLa}_2\text{MnS}_5$ ^[19] synthesized at ambient pressure. This structure type is also reported for some molecular perovskites such as $(\text{NH}_4)\text{CrF}_3$ ^[20] and a disordered form of the famous optoelectronic material $(\text{CH}_3\text{NH}_3)\text{PbI}_3$.^[21] However, Cs_3CoCl_5 -type ternary nitrides have not previously been reported although the oxynitrides $\text{Ln}_3[\text{SiON}_3]\text{O}$,^[22] and $\text{Ho}_3\text{[PN}_4]\text{O}$ ^[23] are known, with the latter displaying the only prior example of a tetrahedral nitride complex in this family. The present work thus demonstrates the importance of the Cs_3CoCl_5 -type structure in high pressure crystal chemistry for stabilization of R_3MN_5 ternary nitrides.

The La_3MnN_5 phases are notable for stabilizing the highest oxidation states of the first row transition metals $\text{M}=\text{Mn}$ and Cr in simple MN_4^{n-} anions. The composition refined from our defect model, $\text{La}_3\text{MnN}_{5.30}$, gives the highest Mn oxidation state (+6.9) yet reported in MnN_4^{n-} nitrido-manganates. The $\text{M}=\text{Cr}$ and Mo analogues contain the highest oxidation state $[\text{MN}_4]^{6-}$ anions which have been reported previously in a few nitridochromates e.g. Li_6CrN_4 ^[24] and Sr_3CrN_4 ,^[25] and a larger number of nitridomolybdates

e.g. Ba_3MoN_4 ^[26] and Na_3MoN_3 containing $[\text{MoN}_2\text{N}_{2/2}]^{3-}$ chains of corner-sharing tetrahedra,^[27] reflecting the greater ease of stabilization of heavy transition metals like Mo in high oxidation states.

It is also notable that La_3MnN_5 was obtained when attempting to synthesise LaMnN_3 perovskite, as perovskites are well-known high pressure phases whereas Cs_3CoCl_5 -types with other anions have not been previously reported as high pressure synthesis products. This may be because the $(\text{MN}_4)\text{NLa}_3$ antiperovskite structure provides greater stabilization of the high oxidation state M^{6+} cations than simple LaMnN_3 perovskite, as it enables each cation to be coordinated by four nitrides in isolated $[\text{M}^{6+}\text{N}_4]^{6-}$ tetrahedra while perovskite has only three nitrides per M^{6+} in the corner-sharing $[\text{M}^{6+}\text{N}_{6/2}]^{3-}$ octahedral network. Furthermore, detailed analysis of the La_3MnN_5 sample suggests that even higher oxidation states can be stabilized through incorporation of extra nitride ions, and the refined composition $\text{La}_3\text{MnN}_{5.296(4)}$ is very close to the theoretical limit of $\text{La}_3\text{Mn}^{7+}\text{N}_{5.33}$.

$\text{La}_3\text{MnN}_{5+x}$ also provides the first report of excess anions in Cs_3CoCl_5 -type antiperovskites, reflecting the high pressure and high nitride activity under synthesis conditions, and it would be interesting to explore whether excess anions can be introduced into the corresponding halides, hydrides, oxides, etc. at pressure or in other ways. Simple ABX_3 antiperovskites are known to accommodate oxide, nitride or carbide at the B sites,^[28] so a further mechanism for tuning oxidation state in antiperovskite nitrides may be through preparation of $(\text{MN}_4)\text{BR}_3$ analogues with B=O or C to respectively stabilize M^{5+} or M^{7+} . The recent report of $(\text{PN}_4)\text{OHO}_3$ ($\text{HO}_3[\text{PN}_4]\text{O}$)^[23] supports such possibilities. Replacement of rare earth by alkaline earth cations may also be used to tune oxidation state, as found with other anions in other Cs_3CoCl_5 -types such as in $\text{BaLa}_2\text{MnS}_5$.^[19]

Conclusion

Three new La_3MN_5 nitrides (M=Cr, Mn and Mo) have been recovered from high pressure and temperature azide synthesis. These are the first examples of ternary Cs_3CoCl_5 -type nitrides, and show that this antiperovskite structure type may be important for stabilisation of high oxidation state transition metal cations in high pressure nitrides. Magnetic measurements confirm that Cr and Mo are in the M^{6+} state, but for Mn an anomalously large cell volume and small paramagnetic moment evidence off-stoichiometry described by an anion-excess $\text{La}_3\text{MnN}_{5.30}$ structure in neutron diffraction analysis where Mn is oxidized almost to Mn^{7+} . This is the first report of incorporation of excess anions in Cs_3CoCl_5 -type materials, and this or other substitution mechanisms may lead to discovery of a large new family of high oxidation state transition metal nitrides.

Supporting Information

The authors have cited additional references within the Supporting Information. Deposition Number 2349641 (for powder neutron refinement of the $\text{La}_3\text{MnN}_{5.3}$ structure) contains the supplementary crystallographic data for this paper. These data are provided free of charge by the joint Cambridge Crystallographic Data Centre and Fachinformationszentrum Karlsruhe Access Structures service.

Acknowledgements

We acknowledge EPSRC for financial support and STFC for the provision of the beamtime at the Institut Laue-Langevin. The authors acknowledge EPSRC for funding. Y. Y. thanks the Talent Training Project of the Dalian Institute of Chemical Physics for support.

Conflict of Interest

The authors declare no conflict of interest.

Keywords: high pressure high temperature · antiperovskite nitride · high oxidation state · sodium azide · magnetic properties

- [1] R. Niewa, G. V. Vajenine, F. J. DiSalvo, H. Luob, W. B. Yelon, *Z. Naturforsch. B* **1998**, *53*, 63–74.
- [2] a) S. D. Kloß, W. Schnick, *Angew. Chem. Int. Ed.* **2019**, *58*, 7933–7944; b) S. Nakamura, T. Mukai, M. Senoh, *Jpn. J. Appl. Phys.* **1991**, *30*, L1998–L2001; c) P. Pust, P. J. Schmidt, W. Schnick, *Nat. Mater.* **2015**, *14*, 454–458; d) P. Pust, V. Weiler, C. Hecht, A. Tücks, A. S. Wochnik, A.-K. Henß, D. Wiechert, C. Scheu, P. J. Schmidt, W. Schnick, *Nat. Mater.* **2014**, *13*, 891–896; e) H. A. Höpfe, H. Lutz, P. Morys, W. Schnick, A. Seilmeier, *J. Phys. Chem. Solids* **2000**, *61*, 2001–2006; f) M. Zeuner, S. Pagano, W. Schnick, *Angew. Chem. Int. Ed.* **2011**, *34*, 7754–7775; g) M. Yang, A. Zakutayev, J. Vidal, X. Zhang, D. S. Ginley, F. J. DiSalvo, *Energy Environ. Sci.* **2013**, *6*, 2994–2999.
- [3] a) A. Salamat, A. L. Hector, P. Kroll, P. F. McMillan, *Coord. Chem. Rev.* **2013**, *257*, 2063–2072; b) R. Kniep, P. Höhn, in *Comprehensive Inorganic Chemistry II (Second Edition): Transition elements, lanthanides and actinides (Volume 2)*, Elsevier **2013**, pp. 137–160.
- [4] S. D. Kloß, A. Haffner, P. Manuel, M. Goto, Y. Shimakawa, J. P. Attfield, *Nat. Commun.* **2021**, *12*, 571.
- [5] S. D. Kloß, J. P. Attfield, *Chem. Commun.* **2021**, *57*, 10427–10430.
- [6] a) S. D. Kloß, M. L. Weidemann, J. P. Attfield, *Angew. Chem. Int. Ed.* **2021**, *60*, 22260–22264; b) S. D. Kloß, C. Ritter, J. P. Attfield, *Allg. Chem.* **2022**, *648*, e202200194.
- [7] K. R. Talley, C. L. Perkins, D. R. Diercks, G. L. Brennecke, A. Zakutayev, *Science* **2021**, *374*, 1488–1491.
- [8] R. Sherbondy, R. W. Smaha, C. J. Bartel, M. E. Holtz, K. R. Talley, B. Levy-Wendt, C. L. Perkins, S. Eley, A. Zakutayev, G. L. Brennecke, *Chem. Mater.* **2022**, *34*, 6883–6893.
- [9] H. M. Powell, A. F. Wells, *J. Chem. Soc.* **1935**, 359–362.
- [10] R. D. Shannon, *Acta Crystallogr. Sect. A* **1976**, *32*, 751–767.

- [11] a) R. S. Nyholm, P. R. Woolliams, D. Shepard, J. Guyer, K. Cohn, *Inorg. Synth.* **1968**, *11*, 56–61; b) R. Olazcuaga, J. M. Reau, G. Leflem, P. Hagenmuller, *Z. Anorg. Allg. Chem.* **1975**, *412*, 271–280.
- [12] R. Niewa, F. R. Wagner, W. Schnelle, O. Hochrein, R. Kniep, *Inorg. Chem.* **2001**, *40*, 5215–5222.
- [13] J. Cabana, N. Dupre, G. Rousse, C. P. Grey, M. R. Palacin, *Solid State Ionics* **2005**, *176*, 2205–2218.
- [14] D. Muller-Bouvet, N. Emery, N. Tassali, E. Panabiere, S. Bach, O. Crosnier, T. Brousse, C. Cenac-Morthe, A. Michalowicz, J. P. Pereira-Ramos, *Phys. Chem. Chem. Phys.* **2017**, *19*, 27204.
- [15] a) O. Tschauer, S. Luo, Y. Chen, A. McDowell, J. Knight, S. Clark, *High Pressure Res.* **2013**, *33*, 202–207; b) D. Laniel, A. Dewaele, G. Garbarino, *Inorg. Chem.* **2018**, *57*, 6245–6251.
- [16] S. S. Jaswal, W. B. Yelon, G. C. Hadjipanayis, Y. Z. Wang, D. J. Sellmyer, *Phys. Rev. Lett.* **1991**, *67*, 644–647.
- [17] W. Bronger, S. Hasenberg, G. Auffermann, *Z. Anorg. Allg. Chem.* **1996**, *622*, 1145–1149.
- [18] G. Liu, J. E. Greedan, W. Gong, *J. Solid State Chem.* **1993**, *105*, 78–91.
- [19] H. Masuda, T. Fujino, N. Sato, K. Yamada, *J. Solid State Chem.* **1999**, *146*, 336–343.
- [20] S. D. Griesemer, L. Ward, C. Wolverton, *Phys. Rev. Mater.* **2021**, *5*, 105003.
- [21] P. Whitfield, N. Herron, W. Guise, K. Page, Y. Cheng, I. Milas, M. Crawford, *Sci. Rep.* **2016**, *6*, 35685.
- [22] a) J. A. Kechele, C. Schmolke, S. Lupart, W. Schnick, *Z. Anorg. Allg. Chem.* **2010**, *636*, 176–182; b) H. A. Höpfe, G. Kotzyba, R. Pöttgen, W. Schnick, *J. Solid State Chem.* **2002**, *167*, 393–401.
- [23] S. D. Kloß, N. Weidmann, W. Schnick, *Eur. J. Inorg. Chem.* **2017**, *2017*, 1930–1937.
- [24] A. Gudat, S. Haag, R. Kniep, A. Rabenau, *Z. Naturforsch. B* **1990**, *45*, 111–120.
- [25] R. Niewa, D. A. Zherebtsov, P. Hoehn, *Z. Kristallogr.* **2003**, *218*, 163.
- [26] a) A. Gudat, P. Höhn, R. Kniep, A. Rabenau, *Z. Naturforsch. B* **1991**, *46*, 566–572; b) M. G. Francesconi, M. G. Barker, P. A. Cooke, A. J. Blake, *J. Chem. Soc. Dalton Trans.* **2000**, 1709–1713.
- [27] P. E. Rauch, F. J. DiSalvo, N. E. Brese, D. E. Partin, M. O’Keeffe, *J. Solid State Chem.* **1994**, *110*, 162–166.
- [28] D. Hirai, H. Tanaka, D. Nishio-Hamane, Z. Hiroi, *RSC Adv.* **2018**, *8*, 42025–42031.

Manuscript received: March 20, 2024

Accepted manuscript online: April 23, 2024

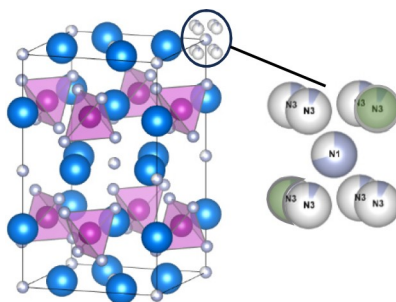
Version of record online: ■■■, ■■■

Communications

Nitride Antiperovskites

Y. Yuan, M. Yang, S. D. Kloß,
J. P. Attfield* [e202405498](#)

A New Family of High Oxidation State
Antiperovskite Nitrides: La_3MN_5 (M=Cr, Mn
and Mo)



La_3MN_5 (M=Cr, Mn, and Mo) are the first examples of ternary antiperovskite (Cs_3CoCl_5 -type) nitrides containing $[\text{MN}_4]^{6-}$ anions for M=Cr and Mo, but for M=Mn off-stoichiometry modelled by excess-nitride clusters gives $\text{La}_3\text{MnN}_{5.30}$ with Mn oxidised almost to the +7 state. This is the first report of excess-anion incorporation into Cs_3CoCl_5 -type materials, and this or other mechanisms may enable many other high oxidation state transition metal nitrides to be prepared.